Numerical Modelling of Slugging Flow in a Gas Fluidised Bed

S. J. Zhang and A. B. Yu
School of Materials Science and Engineering, The University of New South Wales
Sydney, NSW 2052, Australia

ABSTRACT

In this paper, a computational study has been carried out to investigate the slugging behaviour of a fluidised bed using a two-fluid continuum model. Along this approach, gas and solid phases are treated as separate interpenetrating continuum, and the equations are solved for both phases and coupled through their interfacial momentum exchange terms. The computations are started with minimum fluidisation conditions in a rectangular bed. The results are presented in terms of void fraction contours, which can lead to the determination of the slug length and frequency, and the bed expansion.

Keywords: Numerical simulation, two-fluid model, slugging flow, fluidised bed

NOMENCLATURE

C_d	drag coefficient
d_p	diameter of solid particle, m
g	gravity, m/s^2
$G(\varepsilon_s)$	modulus of solid phase, Pa
p	pressure, Pa
Re_p	solid Reynolds number
t	time, s
u_{mf}	minimum fluidisation velocity, m/s
$\mathbf{u}_g$	gas velocity, m/s
$\mathbf{u}_s$	solid velocity, m/s
τ	stress tensor
s	deformation rate tensor

GREEK LETTERS

β	gas-particle momentum transfer coefficient, kg/m^3·s
ε_g, ε_s	gas and solid volume fraction
ε_{mf}	minimum fluidisation porosity
λ_p	mean distance between particles, m
μ_g, μ_s	gas and solid viscosity, kg/m·s
ρ_g, ρ_s	gas and solid density, kg/m^3
ϕ_s	sphericity of the particle

SUBSCRIPT

g	gas
s	solid

1. INTRODUCTION

Gas-particle beds cannot expand indefinitely into ideal, uniform fluidised beds by passing an upward flow of gas through them. Instead they form complex, heterogeneous structures traversed by voids or bubbles. When the size of fluidised beds is relatively small, a bubbling flow in a fluidised bed may evolve into the so-called slugging flow. Stewart and Davidson (1967) describe the two main regimes which can be observed in a fluidised bed when the gas-particle flow is in slug-regime. In the smoothly slugging bed, slugs are round-nosed and solids flow past the slug in an annular region on the wall. This regime occurs with materials which fluidise easily and is contrasted with that in which square-nosed slugs are observed. The square-nosed slugs fill the complete cross-section, solids raining through the slug. The pressure drop across a raining slugging bed is higher and more irregular than across a smoothly slugging bed because of the "locking" of solids on to the bed wall.

However, the presence of the slugs affects the efficiency of interactions as well as the mixing conditions inside the beds, so that the performance of fluidised bed reactors can not be very well predicted without correct gas-particle flow field predictions. Computational method does provide satisfactorily gas-particle flow field in fluidised beds, which should aid in improving the performance of a fluidised bed with slugging flow.

Numerical simulation of gas-particle flow in the fluidised beds was made by several researchers (Gidaspow et al. 1983, Ettehadieh et al. 1984, Bouillard et al. 1989a, 1989b, 1991). All the

previous attempts have concentrated on bubbling fluidisation, but a small amount of efforts (Gidaspow et al. 1991) were also made on the circulating fluidised beds. The specific objective of this numerical investigation is to predict the features of slugging behaviour, such as bed expansion, slug length and frequency, as well as the formation, rise and subsequent breaking of the slugs.

2. GOVERNING EQUATIONS

Hydrodynamic models can be derived by three different methods, The first formulation is reached at intuitively by extending the single-phase equations of conservation. The second approach is researched by using the principles of non-equilibrium thermodynamics (Gidaspow, 1978). But the equations of this model do not as yet include 'second order' terms involving gas and solids viscosities and particle to particle interaction associated with a solid pressure, so it cannot be properly used in dense multi-phase flow. The third approach is obtained by averaging the single-phase conservation equations in a control volume, through space averaging, time averaging or statistical averaging (Soo, 1991). Theoretical treatment favours space averaging while convenient experimental methods favour time averaging. Statistical averaging appears to be convenient in treating general interfaces but it also encounters other some difficulties (Soo, 1991). Presently we use the space averaging approach to obtain the multi-phase continuum model.

The space-averaged continuity and momentum equations for two-dimensional, transient, isothermal, incompressible, viscous flow containing gas and solid phases can be written in the following forms (Jackson, 1985):

(a) the continuity equation for gas phase:

$$\frac{\partial \varepsilon_g}{\partial t} + \nabla \cdot (\varepsilon_g \mathbf{u}_g) = 0 \qquad (1)$$

(b) the continuity equation for solid phase:

$$\frac{\partial \varepsilon_s}{\partial t} + \nabla \cdot (\varepsilon_s \mathbf{u}_s) = 0 \qquad (2)$$

(c) the momentum equation for the gas phase:

$$\frac{\partial(\rho_g \varepsilon_g \mathbf{u}_g)}{\partial t} + \nabla \cdot (\rho_g \varepsilon_g \mathbf{u}_g \mathbf{u}_g) = -\varepsilon_g \nabla p - \beta(\mathbf{u}_g - \mathbf{u}_s) + \nabla \cdot \varepsilon_g \mathbf{t}_l + \rho_g \varepsilon_g \mathbf{g} \qquad (3)$$

(d) the momentum equation for the solid phase:

$$\frac{\partial(\rho_s \varepsilon_s \mathbf{u}_s)}{\partial t} + \nabla \cdot (\rho_s \varepsilon_s \mathbf{u}_s \mathbf{u}_s) = -\varepsilon_s \nabla p - \beta(\mathbf{u}_s - \mathbf{u}_g) + \nabla \cdot \varepsilon_s \mathbf{t}_l + \rho_s \varepsilon_s \mathbf{g} - G(\varepsilon_s)\nabla \varepsilon_s \qquad (4)$$

where

$$\varepsilon_g + \varepsilon_s = 1 \qquad (5)$$

$$\mathbf{t}_l = 2\mu_l \mathbf{s} - 2/3\mu_l \nabla \cdot \mathbf{u}_l \mathbf{I} \quad (l = g \text{ or } s) \qquad (6)$$

$$\mathbf{s} = 1/2[\nabla \mathbf{u}_l + (\nabla \mathbf{u}_l)^T] \quad (l = g \text{ or } s) \qquad (7)$$

In Eq. (4) the additional term $G(\varepsilon_s)\nabla \varepsilon_s$ denoting particle to particle interaction.

In the above equation the significant parameters characterising the behaviour of the bed are the momentum transfer coefficient β, the particle-particle interaction and the solid viscosity μ_s. In general these cannot be treated as constants since they vary with the void fraction in the beds even for a given materials. Hence, additional equations are required to model these parameters, as discussed in the following sections.

3. THE MOMENTUM TRANSFER COEFFICIENT

The drag force between the dispersed particulate phase and the continuous fluid phase is expressed in terms of the product of a momentum transfer coefficient and the relative velocities of the phases.

As the void fraction decreases, indicating an increase in the number density of particles, it is expected that the interface friction force will increase substantially to provide an additional

resistance to the gas flow. The drag relation used in this paper is based on the classical Ergun's equation (1952) which relates the pressure drop in a bed to the superficial gas velocity as follows:

$$-\nabla p_g = [150\frac{\varepsilon_s^2}{\varepsilon_g^3}\frac{\mu_g}{(\phi_s d_p)^2} + 1.75\frac{\varepsilon_s}{\varepsilon_g^3}\frac{\rho_g}{\phi_s d_p}|\mathbf{u}_0|]\mathbf{u}_0 \quad (8)$$

Realising that the superficial velocity, $\mathbf{u}_0 = \varepsilon(\mathbf{u}_g - \mathbf{u}_s)$ and $-\varepsilon_g\nabla p = \beta(\mathbf{u}_g - \mathbf{u}_s)$, the momentum transfer coefficient β is written as

$$\beta = 150\frac{\varepsilon_s^2}{\varepsilon_g}\frac{\mu_g}{(\phi_s d_p)^2} + 1.75\varepsilon_g\frac{\rho_g}{\phi_s d_p}|\mathbf{u}_g - \mathbf{u}_s| \quad (9)$$

The above law is valid for $\varepsilon_g \leq 0.8$. For $\varepsilon_g > 0.8$, Richardson and Zaki (1954) formulated the momentum transfer coefficient as

$$\beta = \frac{3}{4}C_d\frac{\varepsilon_g\varepsilon_s}{\phi_s d_p}\rho_g|\mathbf{u}_g - \mathbf{u}_s|f(\varepsilon_g) \quad (10)$$

where

$$f(\varepsilon_g) = \varepsilon_g^{-2.65} \quad (11)$$

The drag coefficient C_d is related to particle Reynolds number Re_p by

$$C_d = \frac{24}{Re_p}[1 + 0.15(Re_p)^{0.687}] \quad \text{for } Re_p \leq 1000 \quad (12)$$

$$C_d = 0.44 \quad \text{for } Re_p > 1000 \quad (13)$$

where

$$Re_p = \varepsilon_g\rho_g|\mathbf{u}_g - \mathbf{u}_s|d_p/\mu_g \quad (14)$$

4. THE SOLID STRESS AND VISCOSITY

It is necessary to add the solid stress for the solid phase to prevent the particles from reaching impossibly low void fraction. The term is very small in most cases, but becomes of numerical significance when the void fractions go below the minimum fluidisation void fraction. It also helps to make the computation stable, because it converts the imaginary characteristics into real values. The static normal component of this stress, usually called the Coulomb's component, has been used by Concha and Bustos (1987), Gidaspow (1986), and Pritchett et al. (1978).

To place the Coulomb's stress component in perspective, the mechanisms of powder compaction (Shinohara, 1984; Orr, 1966) is considered. The motivation for the most generally satisfactory expression is the experimental observation that plotting the logarithm of consolidating pressure vs. particle volume yields a substantially straight line for both metallic and nonmetallic powders undergoing compaction (Orr, 1966). Orr's (1966) simple theory was used to derive a generalised solid elastic modulus coefficient, $G(\varepsilon)$, of the form

$$G(\varepsilon_s) = G_0\exp[c(\varepsilon_s - \varepsilon_s^*)] \quad (15)$$

where c (called the compaction modulus) is the slope of ln(G) vs. ε_s, and ε_s^* is the compaction solid-phase volume fraction. The normalising units factor, G_0, has been taken to be 1.0 Pa for convenience. For ε_s less than ε_s^*, the exponent of Eq. (15) becomes negative so that the solid elasticity modulus G becomes smaller as ε_s becomes smaller. However, for ε_s greater than ε_s^*, the elasticity modulus G becomes larger as ε_s increases, thus preventing the solid-phase volume fractions from being much larger than ε_s^*. This generalised form of the solid phase elastic modulus, $G(\varepsilon_s)$, has also been incorporated in our computational model, where $c = 230$ and $\varepsilon_s = 56$.

The viscous terms in the momentum equations, although numerically small, introduce a damping effect on the computed values. Pritchett et al. (1978) expressed the solid viscosity as a function of the local void fraction. Ding and

Gidaspow (1990) calculated both the solid phase pressure and viscosity as function of the fluctuating kinetic energy of particles. Following their treatment, Zhang and Yu (1996) also calculated the solid phase pressure and viscosity distributions in a fluidised bed. In this paper, it was assumed to be 0.5 Pa s based on rheological measurement of Grace (1982).

5. COMPUTATIONAL CONDITIONS

To solve the equations of gas-solid flow listed above it is necessary to specify the appropriate boundary conditions for velocities of the solids and the gas, for gas phase pressure, and the void fraction. The void fraction is set to 1 where particle-free gas enters the system. At an impenetrable solid wall, the gas phase velocities in two directions are generally set to zero. This no-slip condition cannot always be applied to solid motion. Since the particle diameter is usually larger than the length scale of surface roughness of the rigid wall, the particle may partially slip at the wall. According to the assumption of Eldighidy et al. (1977), the solid tangential velocity u_{sy} at the wall is proportional to its gradient at the wall, i.e.

$$u_{sy}\big|_w = -\lambda_p \frac{\partial u_{sy}}{\partial x}\Big|_w \qquad (16)$$

where the x direction is normal to the wall. The slip parameter λ_p is known to be the mean distance between particles, and λ_p can be estimated by (Eldighidy et al., 1977)

$$\varepsilon_s \frac{4}{3}\left(\frac{\lambda_p}{2}\right)^3 = \frac{\pi}{6} d_p^3 \qquad (17)$$

This gives

$$\lambda_p = \frac{1}{\varepsilon_s^{1/3}} d_p \qquad (18)$$

Eq. (18) implies that for small particles, the boundary condition is close to the no-slip condition.

The boundary conditions at the symmetric axis demand that gradient of all variables be zero. The inlet conditions for the fluidised bed are indicated in Table 1 such as uniform velocity u_{in} and temperature. At the outlet, the pressure is at an ambient atmosphere and the mass flux is assumed to be continuous.

Initially, the fluidising gas uniformly introduced at the bottom of the bed at the minimum fluidisation velocity, u_{mf}, flows in the vertical y-direction and leaves the bed at the top. At zero time, the uniform velocity of the gas is increased from the minimum fluidisation velocity, u_{mf}, to the required velocity u_{in}. In particular, a freeboard of which height is the 5 times as the bed diameter is provided to allow for bed expansion.

6. RESULTS AND DISCUSSION

The above six nonlinear, coupled, transient, partial differential equations are solved numerically using a finite difference technique. A forward time, centred space discretization is used for temporal and spatial derivatives. The advective terms in the momentum equations are discretized using first-order upwinding. A staggered grid is used in the computations. The velocities for both phases are stored at the cell interfaces, while the pressure and void fractions are stored at the cell centers and the equations are solved for the primitive variables $\mathbf{u}_g$, $\mathbf{u}_s$, p, ε_g and ε_s.

Table 1 Fluidised bed operating conditions used for numerical simulation

Horizontal dimension = 0.2 m
Particle diameter = 500 μm
Initial bed height = 0.3 m
Uniform velocity u_{in} = 1.2 m/s
Ambient pressure = 1 atm
Vertical dimension = 1.3 m
Particle density = 2660 kg/m^3
Min. fluidis. velocity u_{mf} = 0.26 m/s
Min. fluidis. porosity ε_{mf} = 0.44
Temperature = 22°C

A rectangular geometry is used in the calculation, Table 1 shows the typical data used in the computation. Nonuniform finite-difference grids with cell number 13×50 (13 in the x direction and 50 in the y direction) are used in the computation. The time step is 2.5×10^{-4} s. To save computer time, the symmetrical assumption regarding with the centre-line is made. The computations are continued to 7 s of real time.

As suggested above, slugging may occur with large particles in relatively small-diameter fluidised beds. Two major types can be recognised: round-nose and square-nose. Round-nose slugs are present in slugging fluidisation beds consisting of Geldart type A powder. They are in fact 'fast' bubbles that have reached the size of the bed diameter. The particles flow down along side a rising slug and a gas-emulsion interface can be clearly observed. Square-nose slugs occur in slugging beds with particles that show 'slow' bubble behaviour. No clear slug boundary can be observed and particles continuously rain through the void. This type of slug is rather similar to the behaviour of slow bubbles in a bed with large particles. Also, in square-nose slugging, the rise velocity of a gas void is lower than the superficial gas velocity. It has already been concluded by Thiel and Potter (1977) that coarse particles readily form square-nose slugs in high aspect ratio beds of diameter up to 22 cm. From these considerations, it is clear that a small-scale fluidised bed must be in the square-nose slugging flow regime. In this modelling, since in the fluidised bed that is of small diameter with respect to the particle size, square-nose slugging is expected to occur.

Fig. 1 shows numerical results in the two-dimensional fluidised bed. From Fig. 1 it can be seen that at time t = 0.051 s, an almost rectangular slug has detached from the bottom, a sharp lifting of the bed is observed. From the viewpoint of broad concept, it can be regarded as "a large bubble" which is simple as large as the containing tube. In particular the first slug moves up whole across-section and bursts accompanying with merging at its top. There is a down ward motion of the particles at the center of the at later times of the bed and at the walls of the bed. At t = 0.101 s the second slug

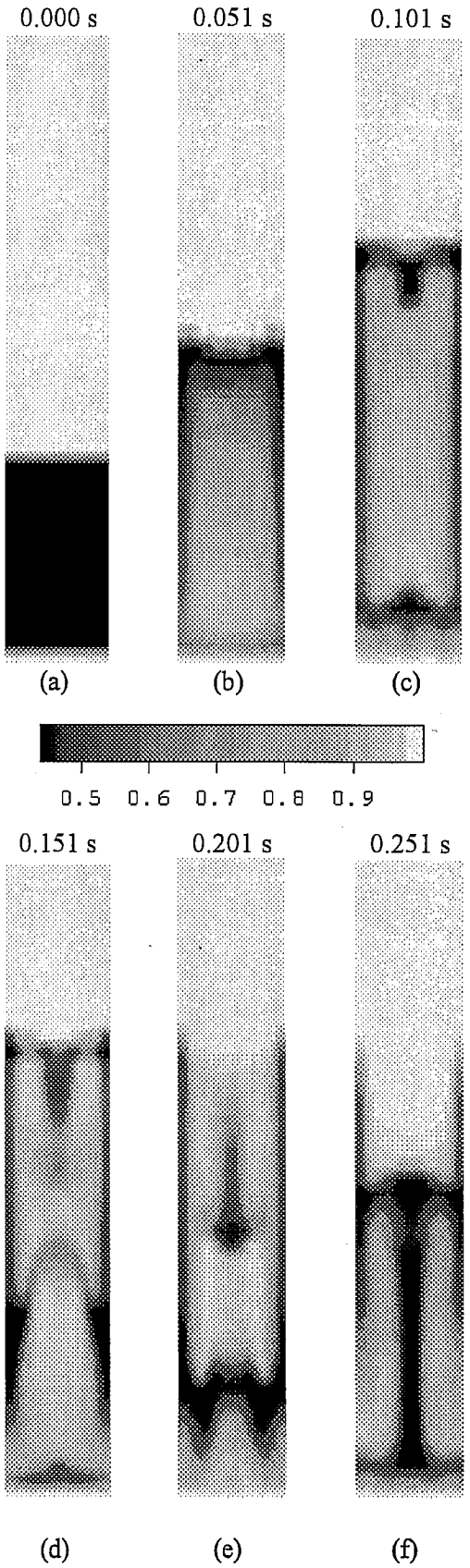

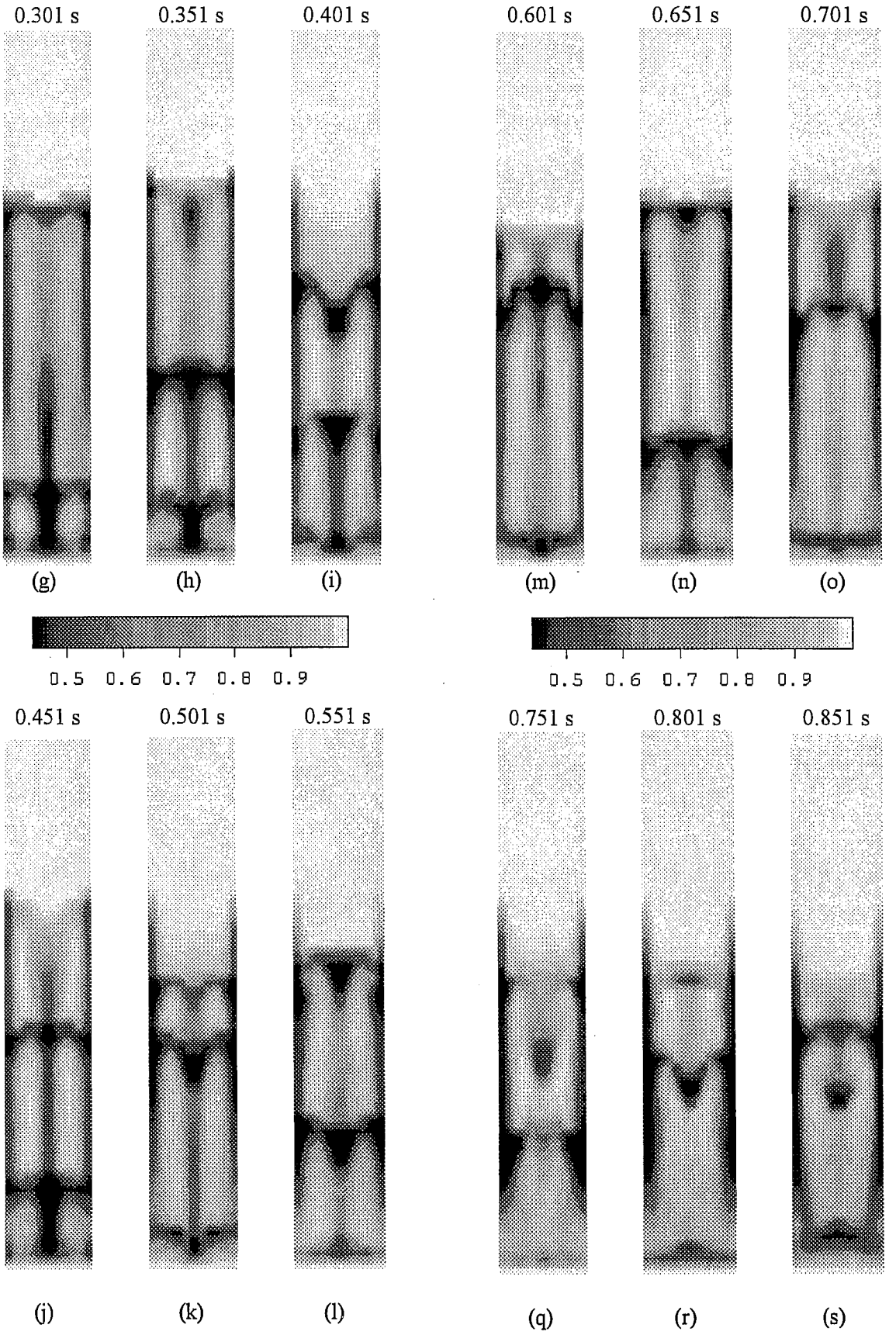

Fig. 1 Shaded void fraction contours at different times

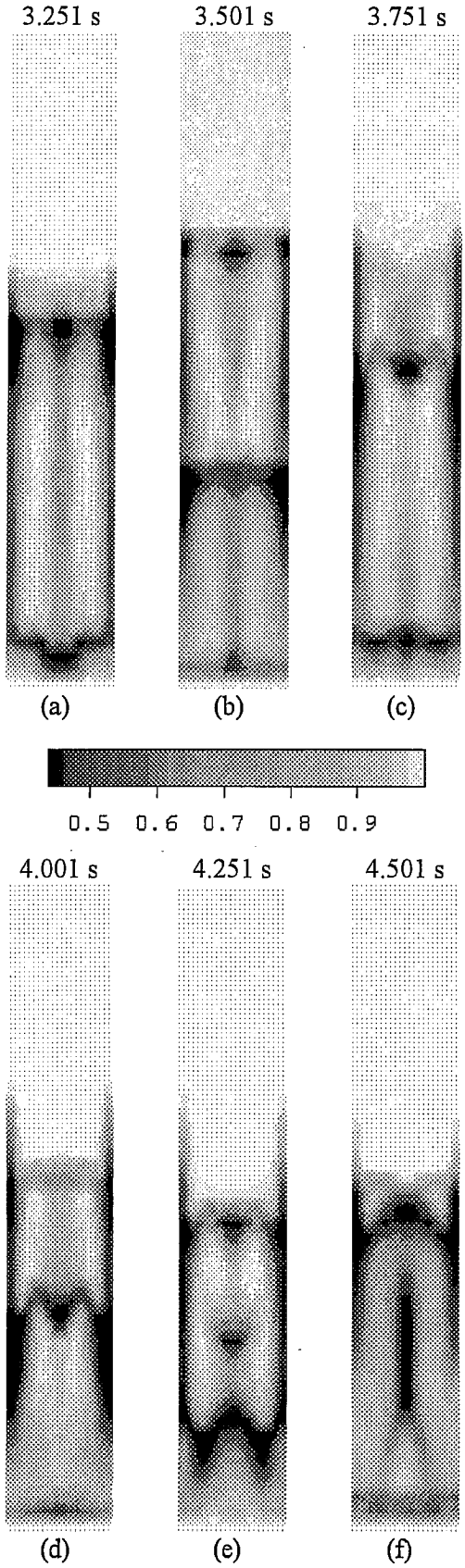

Fig. 2 Shaded void fraction contours

is being formed. At t = 0.151 s the second slug has caught the first slug, broken up the bottom of the first slug, because both slugs run into at the area with the bottom of the first slug and the top of the second slug. Consequently, a comparatively complicated phenomenon is observed. Fig. 1 also shows a number of void fraction shaded contours which clearly illustrate the slug formation in the bed, the resulting expansion of the bed, the slug rise in the bed and the slug eruption at the bed surface. As long as the computation is continued for long enough, it is expected that the long-term behaviour is quite similar under the given conditions, as shown in Fig. 2. The "macroscopic" steady-state can be observed from Fig. 3 and Fig. 4, which shows the porosity variation with times at given points.

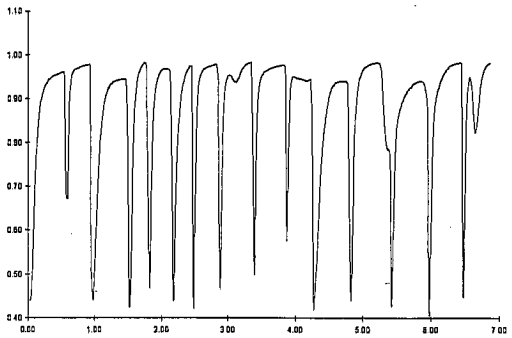

Fig. 3 Porosity oscillation at the position of x = 50 mm, y = 170 mm

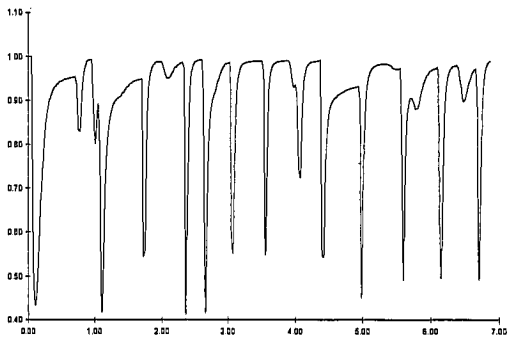

Fig. 4 Porosity oscillation at the position of x = 50 mm, y = 380 mm

7. CONCLUSIONS

A two-fluid model has been developed to simulate the transient dynamics of a slugging fluidised bed for a period of seven seconds. The results demonstrate that the model can predict the formation, rise and eruption of slugs satisfactorily. In the model the behaviour and associated flow pattern of gas and solid phases

in a fluidised bed evolve naturally from numerical computations, with minimum assumptions concerning the gas flow distributor or specification of physical parameters.

REFERENCES

Bouillard, J. X., Lyczkowki, R. W., Folga, S., Gidaspow, D. and Berry, G. F., 1989a, "Hydrodynamics Erosion of Heat Exchanger Tubes in Fluidised Bed Combustors", the Canadian J. Chem. Eng., 67, pp. 218.

Bouillard, J. X., Lyczkowski, R. W. and Gidaspow, D., 1989b, "Porosity Distributions in a fluidised Bed with an Immersed Obstacle", AIChE J. , 35, pp. 908.

Bouillard, J. X., Gidaspow, D. and Lyczkowski, R. W., 1991, "Hydrodynamics of Fluidisation: Fast-Bubble Simulation in a Two-Dimensional Fluidised Bed", Powder Technol., 66, pp. 107.

Concha, F. and Bustos, M. C., 1987, "A Modification of the Kynch Theory of Sedimentation", AIChE J., 33, pp. 312.

Ding, J. and Gidaspow, D., 1990, "A Bubbling Fluidisation Model Using Kinetic Theory of Granular Flow", AIChE J., 36, pp. 523.

Eldighidy, S. M., Chen, R. Y. and Comparin, R. A., 1977, "Deposition of Suspensions in the Entrance of a Channel", J. Fluid Eng., Trans. ASME, June, pp. 365

Ergun, S., 1952, "Fluid Flow Through Packed Columns", Chem. Eng. Prog., 48(2), pp. 89.

Ettehadieh, B., Gidaspow, D. and Lyczkowski, R. W., 1984, "Hydrodynamics of Fluidisation in a Semicircular Bed with a Jet", AIChE J., 30, pp. 529.

Gidaspow, D., 1978, Two Phase Transport and Reactor Safety, T. N. Veziroglu, S. Kakac, eds., Hemisphere Publishing Corp., New York, 1, pp. 283.

Gidaspow, D., 1986, "Hydrodynamics of Fluidisation and Heat Transfer: Supercomputer Modelling", Appl. Mech. Rev., 39, pp. 1.

Gidaspow, D. and Ettehadieh, B., 1983, "Fluidisation in Two Dimensional Beds with a Jet. Part II Hydrodynamics Modelling", Ind. Eng. Chem. Fundam. 22, pp. 193.

Gidaspow, D., Ding, J. and Jayaswal, U. K., 1991, Multiphase Navier-Stokes Solver, Numerical Methods for Multiphase Flows, I. Celik, D. Hughes, C. T, Crown, D. Lankford, eds., pp. 47.

Grace, J. R., 1982, Fluidised-Bed Hydrodynamics, Handbook of Multiphase Systems, G. Hetoroni, ed., Chap. 8.1, McGraw Hill, New York.

Jackson, R, 1985, Hydrodynamic Stability of Fluid-Particle Systems, Fluidisation , J. F. Davidson, R. Clift, D. Harrison, eds., Academic Press, pp. 47.

Orr, Jr. C, 1966, Particulate Technology, Macmillan, New York.

Prichett, J. W., Blake Thomas, R. and Garg, K., 1978, "A Numerical Model of Gas Fluidised Beds", AIChE Symp. Ser. 74, pp. 134.

Richardson, J. F. and Zaki, W. N., 1954, "Sedimentation and Fluidisation: Part I", Trans. Inst. Chem. Eng., 32, pp. 35.

Shinohara, K., 1984, Rheological Property of Particulate Solids, Handbook of Powder Science and Technology, M. E. Fayed and L. Otten, eds., Van Nostrand Reinhold, New York, P129.

Soo, S. L, 1991, "Comparisons of Formulations Multiphase Flow", Powder Technol., 66, pp. 1.

Stewart, P. S. B. and Davidson, J. F., 1967, "Slug Flow in Fluidised Beds", Powder Technol., 1, pp. 61.

Thiel, W. J. and Potter, O. E., 1977, "Slugging in Fluidised Beds", Ind. Eng. Chem. Fundam., 16, pp. 242.

Zhang, S. J. and Yu, A. B., 1996, "Numerical Simulation of Gas-Particle Flow in Dense Fluidised Bed", 5th World Congress of Chemical Engineering, July 14-17, USA, pp. 361.